Asymmetric hydroamination with far fewer chiral species than copper centers achieved by tuning the structure of supramolecular helical catalysts

Paméla Aoun, Ahmad Hammoud, Mayte A Martínez-Aguirre, Laurent Bouteiller, Matthieu Raynal

ARTICLE

Asymmetric hydroamination with far fewer chiral species than copper centers achieved by tuning the structure of supramolecular helical catalysts

Received 00th January 20xx,
Accepted 00th January 20xx

DOI: 10.1039/x0xx00000x

Paméla Aoun, Ahmad Hammoud, Mayte A. Martínez-Aguirre, Laurent Bouteiller, and Matthieu Raynal*

The incorporation of a few chiral monomers (the "sergeants") in a backbone composed of a majority of achiral monomers (the "soldiers") is a well-established strategy to control the handedness of helical polymers. However, the implementation of this "sergeants-and-soldiers" effect in asymmetric catalysis is still at its infancy, with only limited examples for which the sergeant amount is actually in lower amount than the (metal) catalytic unit. Herein, supramolecular co-polymers composed of a benzene-1,3,5-tricarboxamide (BTA) phosphine soldier and a catalytically-inactive BTA sergeant were evaluated in the copper-catalysed hydroamination of styrene. Screening of various BTA ligands revealed the marked influence of substituents on the aryl group of the BTA phosphine ligand, the 3,5-bis-CF_3-substituted ligand providing the highest rate and enantioselectivity. Thorough optimization of the reaction parameters led to a robust protocole for the generation of the amine product in high yield (82±4 %) and moderate *e.e.* (68±6 %). Addition of an achiral BTA additive was found to be beneficial for improving the yield (80-99%), enantioselectivity (up to 81% *e.e.*) and "sergeants-and-soldiers" effect displayed by the supramolecular helical catalyst. Consequently, an enantio-enriched product (75% *e.e.*) was afforded with as low as 0.51 mol% of sergeant in the catalytic mixture, *i.e.* one chiral molecule for 10 copper centers.

Introduction

Although already identified in the sixties[1] on copolymers derived from optically active vinyl monomers,[2] the ability of a few chiral monomers (the "sergeants") to dictate their preferential conformation to a large fraction of achiral monomers (the "soldiers") was unambiguously revealed by Green and co-workers in 1989 during their thorough study of polyisocyanate copolymers.[3] Poly(alkyl isocyanates) adopt helical conformations in solution, which are particularly sensitive to weak chiral influences.[4,5] The "sergeants-and-soldiers" (S&S) effect was remarkable in this class of dynamic helical copolymers[6] since 4% of sergeants yielded a copolymer with an almost single-handed screw sense. This feature was later on observed for a large array of helical covalent polymers,[6,7] helical supramolecular polymers,[8,9] as a well as for discrete assemblies,[10,11] and thermodynamic description of this phenomenon was quantitatively assessed by means of statistical mechanical theory[12] and numerical models.[13]

Implementation of the S&S effect in asymmetric catalysis requires a particular design in which the "soldier" bears a catalytic site and the "sergeant" is catalytically inactive but dictates the preferred handedness of the polymer main chain.[14] A key feature of this relatively new class of asymmetric catalysts is that catalytic centers are intrinsically achiral but experience the chiral environment provided by the helical backbone, which ultimately leads to stereodiscrimination in the transition states. In addition, it represents a unique, yet underexplored, strategy to decrease the amount of chiral inducers in catalytic processes.[15,16] Examples of S&S-type asymmetric catalysts have mainly been reported for helical covalent polymers,[17,18] the most potent ones being based on the poly(quinoxaline-2,3-diyl) (PQX) scaffold.[14,19,20] PQX helical catalysts appended with phosphine ligands were found to provide excellent enantioselectivities in a range of palladium-catalysed reactions, whilst nitrogen-containing PQXs were employed in copper-mediated[21,22] and organocatalytic processes.[23–25] PQX catalysts reported to date either consisted of copolymers embedding a large of fraction of chiral monomers (95%)[26–32] or on terpolymers containing an additional achiral monomer acting as "spacer" between the catalytic unit,[33–36] and for which, the "sergeants" are actually in excess relatively to the catalytic units. Alternatively, external guests[37–40] or solvents[41] can be added in order to induce and memorize a single handedness to helical catalysts but again their loading is large relatively to catalytic units. Transferring the chirality of the sergeant to a large number of catalytic centers is thus an ongoing challenge for S&S-type catalysts.

Since 2013,[42] our group reported examples of S&S-type supramolecular helical catalysts, composed of phosphine-

Sorbonne Université, CNRS, Institut Parisien de Chimie Moléculaire,
Equipe Chimie des Polymères
4 Place Jussieu, 75005 Paris (France)
E-mail: matthieu.raynal@sorbonne-universite.fr

†Electronic Supplementary Information (ESI) available: Supplementary charts, figures and tables, procedure for the preparation of the solutions and catalytic experiments, material and methods, synthesis of BTA ligands, ^{1}H NMR, ESI$^+$ and chiral HPLC spectra. See DOI: 10.1039/x0xx00000x

ARTICLE

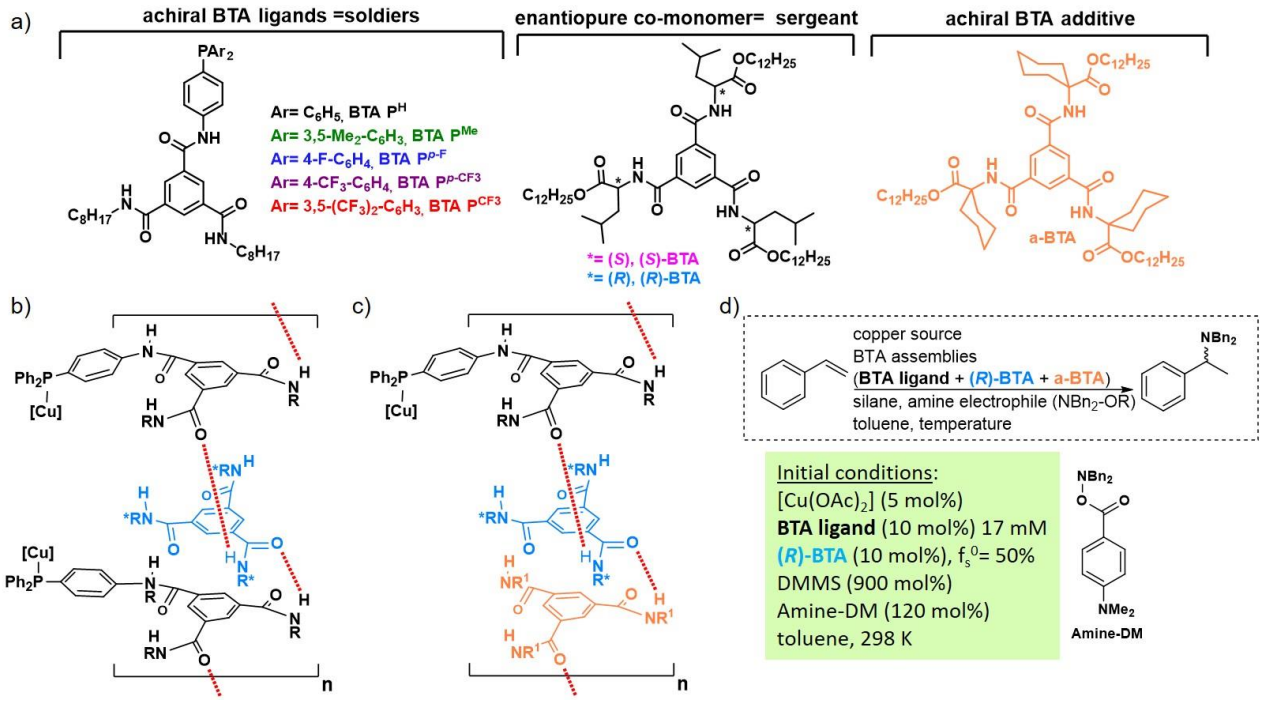

Chart 1 (a) Chemical structures of the BTA monomers employed in this study. (b) Schematic representation of the S&S-type helical assemblies used in the catalytic screening. (c) Schematic representation of the S&S-type helical assemblies operating with low amount of sergeants (high S&S effect). (d) Initial conditions of the catalytic screening.

functionalized and enantiopure monomers, both based on the complementary benzene-1,3,5-tricarboxamide (BTA) scaffold.[43] These examples exploited the well-established S&S effect observed in BTA helical assemblies[44–48] and in related discotic monomers.[49] It was notably possible to perform the rhodium-catalysed hydrogenation of dimethyl itaconate with a copolymer composed of one sergeant for two rhodium centers on average, thus representing the first example for which a sub-stoichiometric amount of a chiral inducer was used relatively to the metal catalyst, without significant deterioration of the enantioselectivity.[50] The catalytic mixture between **BTA P^{H}** (Chart 1a) and a sergeant (as represented in Chart 1b) was also evaluated in the copper-catalysed hydrosilylation of acetophenone derivatives,[51–53] but in that case, efficient S&S effect was observed only if a third co-monomer (**a-BTA**) was also present in the helical assemblies (Chart 1c). It was found that **a-BTA** both stabilize the assemblies and remove the conformational defects thus allowing efficient hydrosilylation of 4-nitroacetophenone in 90% enantiomeric excess (*e.e.*) at 200 K and as low as 0.25% of sergeant in the mixture.[54] Extending the scope of this highly efficient S&S effect requires to probe its validity with other soldier structures and under different reaction conditions. Herein, we report our efforts dedicated to the implementation of S&S-type BTA helical catalysts in the copper-catalysed hydroamination of styrene, a reaction that proved to be efficiently catalysed by conventional chiral diphosphine ligands.[55–57] Selection of the best-performing BTA ligand partner (the "soldier") and thorough screening of the experimental conditions afforded the amine product in 75% *e.e.* with as low as 0.51 mol% of sergeant in the catalytic mixture, *i.e.* one chiral molecule for 10 copper centers.

Results and discussion

Design and synthesis of BTA monomers. The asymmetric Cu-H promoted hydroamination of alkenes[55–57] is performed efficiently by a relatively narrow number of chiral diphosphine ligands,[58–83] with particularly strong effects exerted by substituents located on the aryl rings attached to the phosphorus atom.[84,85] In addition to BTA ligands, **BTA P^{H}** and **BTA P^{Me}**, previously investigated in the copper-catalysed hydrosilylation of acetophenone derivatives,[51,52,54] it appears desirable to investigate more electron poor ligands as it may facilitate the hydrocupration step of the catalytic cycle.[85] Accordingly, **BTA P$^{p\text{-}F}$**, **BTA P$^{p\text{-}CF3}$** and **BTA P^{CF3}** (Chart 1a) were prepared following previously established procedures and characterized by conventional techniques (ESI†). Initially screened co-assemblies were composed of one of these BTA

ARTICLE

Table 1 Characterization of the helical co-assemblies for the S&S-type mixtures between **(*R*)-BTA** and the different BTA ligands. [BTA ligand]= 3.33 g.L^{-1} in toluene-d_8 except for SANS analysis of **BTA P^{H}** mixture (4.0 g.L^{-1}).

BTA ligand in the S&S-type mixtures	f_s^0 (%)[a]	BTA in stacks (%)[b]	f_s^s-SANS (%)[c]	f_s^s-IR (± 1%)[c]	|g| value at maximum (10^{-4})[d]
BTA P^{H}	39	86±3	35±4	30	6.8
BTA P^{Me}	41	81±2	28±6	28	5.2
BTA P$^{p\text{-}F}$	41	88±2	*nd*	32	7.7
BTA P$^{p\text{-}CF3}$	44	86±3	*nd*	34	7.1
BTA P^{CF3}	47	86±3	31±6	39	6.5

(a) f_s^0= fraction of sergeant introduced into the solution= [**(*S*)-BTA**]^0/([**(*S*)-BTA**]^0 + [BTA ligand]^0). (b) Molar fraction of BTA in stacks= ([BTA ligand]^0+[**(*R*)-BTA** in stacks determined by FT-IR])/(total BTA concentration). **(*R*)-BTA** monomers that are not in the stacks form dimers (ESI†).[86–88] (c) f_s^s= fraction of sergeant in stacks as determined by SANS (f_s^s-SANS) or by FT-IR (f_s^s-IR) analyses. f_s^s= ([**(*R*)-BTA** in stacks]/([**(*R*)-BTA** in stacks] + [BTA ligand]^0). (d) Kuhn anisotropy factor (g) was measured at the maximum of CD signals (close to 300 nm in all cases). By comparison with the g_{max} value previously determined for homochiral assemblies of **BTA P^{H}** (≈ 7.0× 10^{-4}),[54] it can be surmised a relatively high optical purity of the supramolecular helices for all mixtures. *nd*= not determined

ligands and of **(*R*)-BTA** (resp. **(*S*)-BTA**) as the latter component has demonstrated its ability to intercalate into the helical assemblies of the BTA ligands[53] and induce a preferred left- (resp. right) handedness to the supramolecular co-assemblies (Chart 1b).[51]

Characterization of the S&S-type co-assemblies. Prior to catalytic screening, we determined the composition, geometry and chiroptical properties of the BTA ligand homo-assemblies and of the S&S-type co-assemblies following our previously established analytical procedure.[51–53,87] Indeed, depending on their structure and on the conditions, BTAs can either self-assemble into stacks or into dimers,[86–88] but only the stacks can be expected to show strong S&S effects. Fourier-transform Infrared (FT-IR, Figures S1-S2) analyses indicated that all BTA ligands form long hydrogen-bonded stacks.‡ Mixtures containing the different BTA ligands (3.33 g.L^{-1}) and **(*R*)-BTA** (39%≤ f_s^0≤ 47%, Table 1) were analysed in toluene-d_8, a suitable solvent for both assemblies' formation and catalysis. Small-Angle Neutron Scattering (SANS) analyses (Figure S3) are consistent with long (length> 27 nm *i.e.* DP_n> 35) and one-dimensional objects. **(*R*)-BTA** monomers are incorporated into the stacks of the BTA ligands as indicated by FT-IR and SANS analyses. Most of the BTA monomers in these S&S-type mixtures are actually present in the stacks (BTA in stacks≥ 81%, Table 1). The fraction of **(*R*)-BTA** monomers (sergeants) in the stacks, f_s^s, can be accurately determined, with similar results deduced independently from FT-IR and SANS analyses, and is found to be close to the fraction of **(*R*)-BTA** monomers initially introduced into the mixtures (compare f_s^0 and f_s^s in Table 1). This means that **(*R*)-BTA** efficiently intercalates[53,89,90] into the stacks of the BTA ligands leading to the formation of long helical co-assemblies. Circular dichroism (CD) analyses (Figure S4a) revealed a negative band with a maximum around 300 nm for all S&S-type mixtures. This band, which belongs to the BTA ligand only (Figure S4b), is an induced CD (ICD) band[91] and thus reflects the chiral environment experienced by the ligand in the helical co-assemblies. By analogy with the **BTA P^{H}** containing mixture, it can be inferred that all co-assemblies are left-handed[51] and possess a relatively high optical purity (see g values, Table 1).[54] Overall, the combination of FT-IR, SANS and CD analyses indicates that the PAr_2 moiety in this BTA ligand series has thus no significant influence on the structure of the helical co-assemblies. A subtle effect can be detected for the **BTA P^{Me}** mixture which exhibits a lower g value as a probable result of a slightly lower amount of sergeants incorporated into the stacks, relatively to other co-assemblies. Likewise, the ICD band displayed by the **BTA P^{CF3}** mixture (Figure S4a) has a slightly different shape with two extrema at 285 and 305 nm instead of a single one at *ca.* 300 nm for all the other mixtures. This might be due to a subtle difference in the conformation adopted by the 3,5-bis-CF_3-substituted PAr_2 moiety. Finally, it is important to note that no significant change of the structure of the co-assemblies is expected upon copper binding,[52] thus co-assemblies can be schematically represented as shown in Chart 1b. Although the precise coordination mode of the copper centers at the periphery of the helices cannot be ascertained, the formation of long and predominantly one-handed helical co-assemblies whatever the nature of the BTA ligand motivates their evaluation in catalysis.

Influence of BTA ligand in the copper-catalysed hydroamination of styrene. Initial conditions for the evaluation of the different S&S-type helical catalysts were selected as follows: i) a concentration in BTA ligand of 17 mM to ensure the presence of sufficiently long assemblies, ii) a fraction of sergeants of 50% to promote the formation of single-handed helices, iii) **Amine-DM** to minimize the detrimental direct reduction of the amine electrophile by Cu-H species,[60,92] and iv) a high concentration in dimethoxy(methyl)silane (DMMS) to increase the reaction rate[61] and provide a sufficient amount in *N*,*N*-dibenzyl-1-phenylethanamine (DBA) whatever the ligand present in the S&S-type mixtures. The reactions were monitored by ^{1}H NMR

ARTICLE

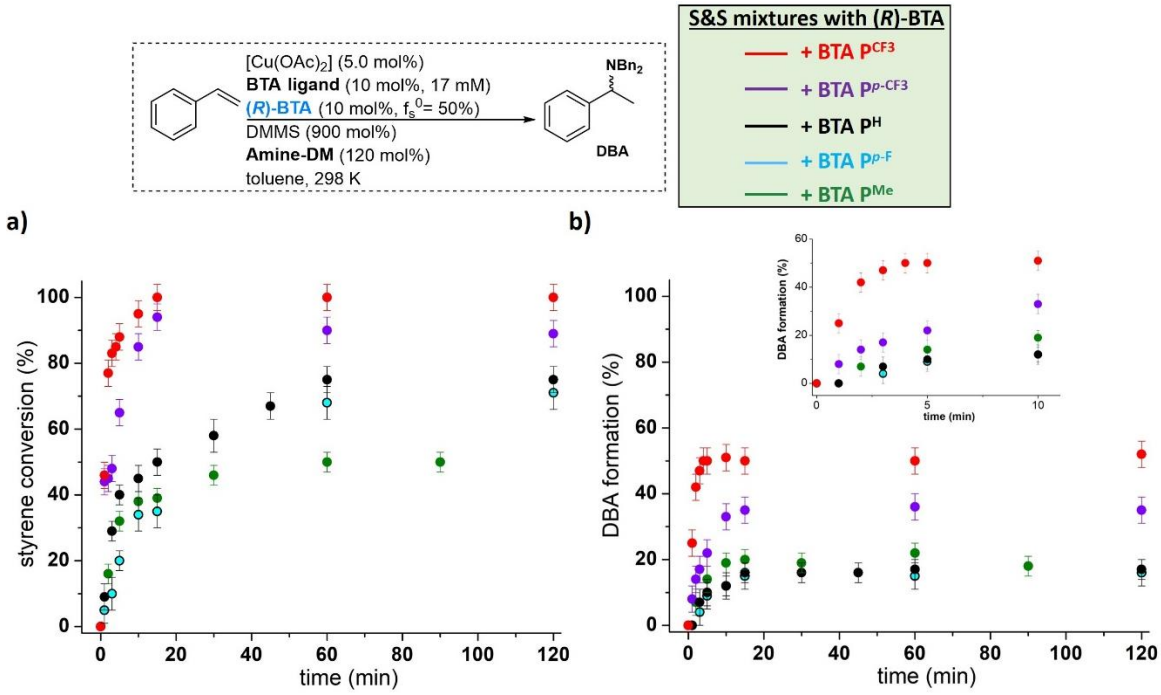

Figure 1 Influence of the BTA ligand in the copper-catalysed hydroamination of styrene. (a) Conversion of styrene (a) and DBA formation (b) versus time. Inset: reaction points at the onset of the reaction.

Table 2 Catalytic results in the copper-catalysed hydroamination of styrene for the different S&S-type mixtures.

BTA ligand in the S&S-type mixtures	styrene conversion (± 5%)[a]	initial rate (10^{-3} M.min^{-1})[b]	DBA yield (±4 %)[c]	DBA *e.e.* (±1 %)[d]
BTA P^{H}	75	3.8	17	29 (*R*)
BTA P^{Me}	50	4.7	22	58 (*R*)
BTA $P^{p\text{-}F}$	71	3.2	16	19 (*R*)
BTA $P^{p\text{-}CF3}$	94	12	36	7 (*R*)
BTA P^{CF3}	100	36	52	68 (*R*)

(a) Styrene conversion after 120 minutes. Error bar according to integration of the different styrene signals. (b) Initial rate corresponding to the derivative of the reaction points at the onset of the reaction. (c) NMR yield measured after 120 minutes, relatively to the internal standard. Error bar according to integration of DBA signals. (d) The optical purity of DBA was determined by chiral HPLC analysis and configuration of the DBA enantiomers was established according to the literature.[55,61] Error bar according to integration of HPLC signals.

with 1,3,5-trimethoxybenzene as an internal standard and the results are plotted in Figure 1 (see Figures S5 to S9 for the NMR spectra). All helical catalysts promote rapid consumption of styrene and formation of DBA at the onset of the reaction followed by rapid plateauing of the reaction progress. This might be explained by rapid consumption of the reactants, including **Amine-DM** (ESI†), and possibly catalyst deactivation.[85] Whatever the ligand, styrene is only partly transformed into DBA: i) ethylbenzene, presumably formed by hydrolysis of the alkyl copper intermediate,[78] is detected in 10±5% in each mixtures (Figure S10) and ii) alternative hydrofunctionalization processes, such as styrene hydrosilylation,[93] constitute other potential side reactions.

The nature of the BTA ligand strongly influences the outcome of the catalytic reaction (Table 2). CF_3 substituted ligands, **BTA $P^{p\text{-}CF3}$** and **BTA P^{CF3}**, provided DBA with higher rates relatively to other ligands probably because the hydrocupration step is facilitated in these systems. All S&S-type helical catalysts furnish **(*R*)-DBA** as the major enantiomer, as expected from their same sense of rotation (*vide supra*), however with markedly different optical purities. Ligands with substituents at the *meta* positions of the phosphine aryl rings, **BTA P^{Me}** and **BTA P^{CF3}**, give significantly higher enantioselectivities than the non-modified

ARTICLE

Table 3 Catalyst optimization.

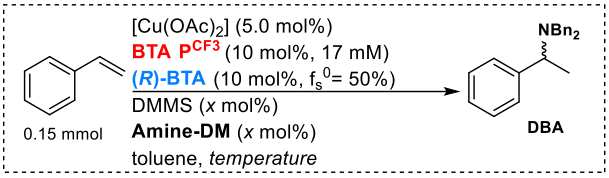

Entry	DMMS (*x* mol%)	**Amine-DM** (*x* mol%)	Temperature (K)	DBA yield (± 4%)[a]	DBA *e.e.* (%)
1	900	120	298	52	68 (*R*)
2	400	120	298	42	69 (*R*)
3	400	120	313	82	68±6[b] (*R*)
4	400	120	333	75	63 (*R*)
5	400	180	313	93	69 (*R*)
6	400	180	313	93	69 (*S*)[c]

(a) NMR yield measured relatively to the internal standard. Error bar according to integration of DBA signals**.** (b) The entry was repeated 9 times, yielding the following *e.e.* values: 73%, 65%, 67%, 65%, 63%, 68%, 73%, 70% and 69%. Based on this repeatability assessment, a mean *e.e.* value of 68% can be deduced as well as an error bar of ±6% (equals to ±½ variance). Corresponding NMR yields are**:** 83%, 80%, 80%, 84%, 83%, 80%, 80%, 84% and 80% providing a mean yield of 82% with ±2% error bar (within the experimental error of NMR integration). (c) **(*S*)-BTA** was used instead of **(*R*)-BTA**.

ligand (**BTA P^{H}**) and substitution at the *para* position appears to be detrimental for the enantioselectivity. Modelling of transition states with chiral diphosphine Cu-H complexes have revealed the importance of through-bond and through-space interactions between the ligand and substrate for accelerating the hydrocupration step.[84,85] It is plausible that these interactions also affect the selectivity of the enantio-determining step, as observed here. Undeniably, the helical catalyst composed of **BTA P^{CF3}** and **(*R*)-BTA** is the most efficient investigated system for the copper-catalysed hydroamination of styrene.

Catalyst optimization. A range of parameters were screened to improve the catalytic performance of the helical catalyst based on the **BTA P^{CF3}** ligand (Tables S1.1 to S1.5). Parameters that led to significant improvement of the catalytic system relatively to initial conditions (entry 1) are shown in Table 3. The amount of DMMS can be decreased to 400 mol% with only a small erosion of the DBA yield (entry 2). Performing the reaction at 313 K leads to a greater DBA yield (82%) without dwindling of the enantioselectivity (entry 3). The reaction was repeated 9 times under these conditions providing fairly reproducible DBA yield (82±2 %) and *e.e.* (68±6 %). Screening of various copper sources (Table S1.2), copper/ligand ratios (Table S1.2), silanes (Table S1.3) and amine electrophiles (Table S1.4) does not lead to further improvement. Further increase of the temperature to 333 K neither proves to be beneficial (entry 4). It is interesting to note that the concentration in **BTA P^{CF3}** can be advantageously decreased down to 5 mM with no alteration of the catalytic performance (Table S1.5). Implementation of these modified conditions to **BTA P^{Me}**-containing helical catalyst does not have a similar effect; low yields (*ca.* 20%) are obtained whatever the conditions (Table S2).

Finally, the yield in DBA is further improved by adding a larger excess of **Amine-DM** (entry 5), thus minimizing the extent of competing side reactions. When the reaction was conducted in presence of **(*S*)-BTA** instead of **(*R*)-BTA**, the opposite enantiomer of DBA is obtained with the same selectivity (entry 6), as expected since these S&S-type helical catalysts exhibit opposite handedness. A larger scale catalytic experiment (0.45 mmol) allowed the isolation of pure DBA in 60% yield and 64% *e.e.* (Figure S11).

Asymmetric hydroamination with low amount of sergeants. Benefiting from the aforementioned screening of operating parameters, the catalytic hydroamination of styrene was performed with fractions of **(*S*)-BTA** (relatively to achiral monomers) ranging from 0.26% to 50%, which correspond to catalytic loadings (relatively to styrene) comprised between 0.05 mol% and 20 mol% (see Table S3 for the exact compositions). DBA isolated yields and *e.e.* values for reactions in presence and absence of **a-BTA** as the achiral additive[54] are plotted in Figure 2. In presence of 0.10 mol% of **(*S*)-BTA**, the mixture lacking **a-BTA** exhibits low yield (22%) and *e.e.* (10%). The low yield is likely the result of the limited solubility[‡] of this

ARTICLE

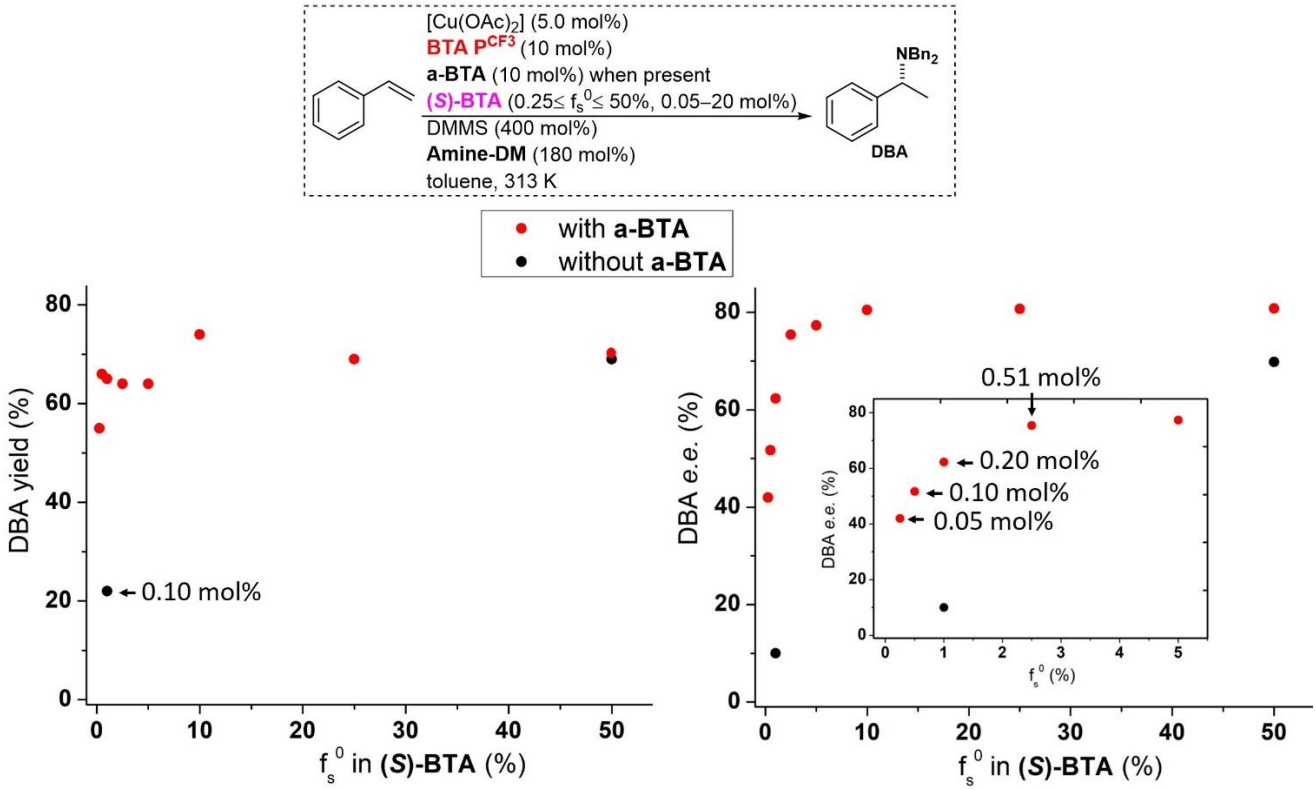

Figure 2 DBA isolated yield (left) and *e.e.* (right) for S&S-type catalytic experiments performed with **BTA P^{CF3}** and various amounts of **(*S*)-BTA**, in presence or absence of **a-BTA**. Inset: zoom on the region of low f_s^0 values, catalytic loading in **(*S*)-BTA** is indicated for selected points. f_s^0= fraction of sergeant introduced into the solution= [**(*S*)-BTA**]^0/([**(*S*)-BTA**]^0 + [**BTA P^{CF3}**]^0 + [**a-BTA**]^0).

mixture at low **(*S*)-BTA** fractions whereas the low *e.e.* value is indicative of the absence of S&S effect. In sharp contrast, uniform NMR yields (80-99%) and isolated yields (55%-74%) are observed when the reactions are conducted in presence of **a-BTA**, whatever the amount of **(*S*)-BTA**. In addition, the effect of **a-BTA** on the enantioselectivity in DBA shows the anticipated hallmark of a high S&S effect: *e.e.* values around 80% are maintained for fraction of **(*S*)-BTA** as low as 2.5%. From there, the selectivity decreases smoothly to 42% for f_s^0= 0.26%. The magnitude of the S&S effect is remarkable relatively to previously reported helical catalysts,[33–36] but yet lower than that observed for the hydrosilylation of 4-nitroacetophenone with a related BTA system (optimal selectivity reached for f_s^0= 0.5%).[54] It is possible that a larger fraction of defects is present in the hydroamination catalyst as the result of a higher temperature required for efficient DBA formation.[48] Remarkably, the selectivity in DBA is also higher for the three-component system allowing to reach up to 81% *e.e.* versus 68±6% *e.e.* for the two-component one. Interestingly, an opposite effect was observed for the hydrosilylation reaction, *i.e.* sergeant-rich three-component mixture yielded lower selectivity.[54] This likely originates from a subtle change in the conformation of **BTA P^{CF3}** in presence of **a-BTA** as confirmed by different CD signatures of the three- and two-component BTA systems (Figure S12). These beneficial effects of the achiral additive allow DBA to be isolated in reasonable yield (55%) and 42% *e.e.* with as low as 0.05 mol% of **(*S*)-BTA**, *i.e.* one chiral molecule for 100 copper centers. Increasing the sergeant to copper ratio to 1/10 affords DBA in 64% yield and 75% *e.e.*, *i.e.* better catalytic results than with a sergeant/copper ratio of 1 in absence of **a-BTA**. These results indicate that, in contrast to conventional organometallic catalytic systems, the optimal enantioselectivity of helical BTA catalysts can also be tuned by achiral additives that do not directly interact with coordination spheres of the metal centre.[94,95]

Conclusion

Guiding rules are necessary to further exploit sergeants-and-soldiers-type helical systems in asymmetric catalysis. The

present work demonstrates that the recently disclosed ability of an achiral benzene-1,3,5-tricarboxamide additive, **a-BTA**, to dramatically increase the magnitude of the S&S effect in the Cu-H catalysed hydrosilylation[54] is also valid for the hydroamination reaction, even though more drastic conditions (313 K, excess of amine electrophile reagent) is required for this reaction to proceed efficiently. The combination of **a-BTA** and optimized reaction conditions affords the hydroamination product with reasonable yield (69%) and *e.e.* (81%). The effect of **a-BTA** is actually threefold since it proves to be beneficial not only for the magnitude of the S&S effect (close to optimal selectivity with as low as 0.51 mol% of sergeant) but also for the yield and enantioselectivity of the catalytic process. It motivates easily assembled multi-component BTA helical systems to be investigated in related Cu-H reactions[55–57] as well as different catalytic transformations.

Experimental

Sergeants-and-soldiers experiments with **BTA P^{CF3}** [9.6 mM], **a-BTA** [9.6 mM], and **(*S*)-BTA**: an oven-dried test tube was loaded with **BTA P^{CF3}** (43.4 mg, 45.0 µmol, 10.0 mol%), $[Cu(OAc)_2]$ (4.1 mg, 22.5 µmol, 5.0 mol%) and dry THF (500 µL). The solvent was removed under vacuum and the tube was kept under vacuum (10^{-3} mbar) for 1 hour. **(*S*)-BTA** (0.23–90 µmol, 0.05–20.0 mol%), **a-BTA** (49.1 mg, 45.0 µmol, 10.0 mol%), and toluene (4000 µL) were added to the tube and the mixture was briefly heated to reflux and stirred for 15 minutes at room temperature. Styrene (51 µL, 0.45 mmol, 100 mol%), and **Amine-DM** (292 mg, 0.81 mmol, 180 mol%) were added to the tube and the tube was flushed with argon for 10 seconds. The reaction mixture was heated to 40°C and DMMS was added (223 µL, 1.8 mmol, 400 mol%). After 2 hours, the reaction mixture was cooled down to room temperature and 2 mL of a saturated aqueous solution of Na_2CO_3 was added as well as ethyl acetate (1 mL). The phases were separated and the aqueous layer was extracted with ethyl acetate (2×1 mL). 1,3,5-trimethoxybenzene (75.7 mg, 0.45 mmol, 100 mol%) was added to the combined organic phases and the NMR yield was established after evaporation of the solvent. Acetonitrile was added to the crude and the insoluble material was discarded by filtration. The crude material was purified by flash column chromatography over silica gel, eluting with dichloromethane/ethyl acetate yielding **(*S*)-DBA** as a colourless oil (see isolated yields in Table S.3). The optical purity of DBA in each sergeants-and-soldiers mixture was determined by chiral HPLC. For additional experimental procedures, see the ESI†.

Author Contributions

Conceptualization: M.R.; supervision: M.R. and L.B.; characterization of the co-assemblies: L.B., A.H. and M. M.-A.; screening of the BTA ligands: A.H. and P.A.; optimization of the reaction conditions: P.A.; S&S-type experiments: M. M.-A.; writing – original draft: M.R. All authors participated to the edition of the final version of the manuscript.

Conflicts of interest

There are no conflicts to declare.

Acknowledgements

This work was supported by the French Agence Nationale de la Recherche (project ANR-17-CE07-0002 AbsoluCat, Ph.D. grant of A.H., PDRA grant of P.A.) and by the Consejo Nacional de Ciencia y Tecnologia (CONACYT, PDRA grant of M. M.-A.). Jacques Jestin (LLB, Saclay) and Omar Khaled (IPCM, Sorbonne Université) are acknowledged for assistance with SANS and chiral HPLC experiments, respectively. Lucrèce Matheron-Duriez and Gilles Clodic are acknowledged for the ESI analysis of catalytic samples.

Notes and references

‡ BTA ligand, **BTA P^{CF3}**, was not soluble on its own in toluene-d_8 and thus only co-assemblies formed in presence of **(*R*)-BTA** have been characterized. Likewise, good solubility of this two-component mixture is obtained at the condition that sufficient amount of **(*S*)-BTA** ($f_s^0 \geq 25\%$) is present in the mixture.

1 C. Carlini, F. Ciardelli and P. Pino, *Makromol. Chem.*, 1968, **119**, 244–248.
2 F. Ciardelli and P. Salvadori, *Pure Appl. Chem.*, 1985, **57**, 931–940.
3 M. M. Green, M. P. Reidy, R. D. Johnson, G. Darling, D. J. O'Leary and G. Willson, *J. Am. Chem. Soc.*, 1989, **111**, 6452–6454.
4 M. M. Green, C. Andreola, B. Munoz, M. P. Reidy and K. Zero, *J. Am. Chem. Soc.*, 1988, **110**, 4063–4065.
5 M. M. Green, J.-W. Park, T. Sato, A. Teramoto, S. Lifson, R. L. B. Selinger and J. V. Selinger, *Angew. Chem. Int. Ed.*, 1999, **38**, 3138–3154.
6 E. Yashima, K. Maeda, H. Iida, Y. Furusho and K. Nagai, *Chem. Rev.*, 2009, **109**, 6102–6211.
7 E. Yashima, N. Ousaka, D. Taura, K. Shimomura, T. Ikai and K. Maeda, *Chem. Rev.*, 2016, **116**, 13752–13990.
8 A. R. A. Palmans and E. W. Meijer, *Angew. Chem. Int. Ed.*, 2007, **46**, 8948–8968.

9 M. Liu, L. Zhang and T. Wang, *Chem Rev*, 2015, **115**, 7304–7397.
10 L. J. Prins, J. Huskens, F. de Jong, P. Timmerman and D. N. Reinhoudt, *Nature*, 1999, **398**, 498–502.
11 Y. Lei, Q. Chen, P. Liu, L. Wang, H. Wang, B. Li, X. Lu, Z. Chen, Y. Pan, F. Huang and H. Li, *Angew. Chem. Int. Ed.*, 2021, **60**, 4705–4711.
12 J. van Gestel, P. van der Schoot and M. A. J. Michels, *Macromolecules*, 2003, **36**, 6668–6673.
13 A. J. Markvoort, H. M. M. ten Eikelder, P. A. J. Hilbers, T. F. A. de Greef and E. W. Meijer, *Nat. Commun.*, 2011, **2**, 509.
14 Y. Li, L. Bouteiller and M. Raynal, *ChemCatChem*, 2019, **11**, 5212–5226.
15 Z. Shen, Y. Sang, T. Wang, J. Jiang, Y. Meng, Y. Jiang, K. Okuro, T. Aida and M. Liu, *Nat. Commun.*, 2019, **10**, 1–8.
16 A. Arlegui, B. Soler, A. Galindo, O. Arteaga, A. Canillas, J. M. Ribó, Z. El-Hachemi, J. Crusats and A. Moyano, *Chem. Commun.*, 2019, **55**, 12219–12222.
17 M. Reggelin, S. Doerr, M. Klussmann, M. Schultz and M. Holbach, *Proc. Natl. Acad. Sci.*, 2004, **101**, 5461–5466.
18 L. M. S. Takata, H. Iida, K. Shimomura, K. Hayashi, A. A. dos Santos and E. Yashima, *Macromol. Rapid Commun.*, 2015, **36**, 2047–2054.
19 M. Suginome, T. Yamamoto, Y. Nagata, T. Yamada and Y. Akai, *Pure Appl. Chem.*, 2012, **84**, 1759–1769.
20 M. Suginome, T. Yamamoto and Y. Nagata, *J. Synth. Org. Chem. Jpn.*, 2015, **73**, 1141–1155.
21 Y. Yoshinaga, T. Yamamoto and M. Suginome, *ACS Macro Lett.*, 2017, **6**, 705–710.
22 Y. Yoshinaga, T. Yamamoto and M. Suginome, *J. Am. Chem. Soc.*, 2020, **142**, 18317–18323.
23 T. Yamamoto, R. Murakami and M. Suginome, *J. Am. Chem. Soc.*, 2017, **139**, 2557–2560.
24 T. Yamamoto, T. Takahashi, R. Murakami, N. Ariki and M. Suginome, *Bull. Chem. Soc. Jpn.*, 2021, **94**, 943–949.
25 T. Yamamoto, R. Murakami and M. Suginome, *Org. Lett.*, , DOI:10.1021/acs.orglett.1c03134.
26 T. Yamamoto, T. Yamada, Y. Nagata and M. Suginome, *J. Am. Chem. Soc.*, 2010, **132**, 7899–7901.
27 Y. Nagata, T. Nishikawa and M. Suginome, *J. Am. Chem. Soc.*, 2014, **136**, 15901–15904.
28 Y. Nagata, T. Kuroda, K. Takagi and M. Suginome, *Chem. Sci.*, 2014, **5**, 4953–4956.
29 Y. Akai, L. Konnert, T. Yamamoto and M. Suginome, *Chem. Commun.*, 2015, **51**, 7211–7214.
30 T. Yamamoto, Y. Akai and M. Suginome, *Angew. Chem. Int. Ed.*, 2014, **53**, 12785–12788.
31 Y. Akai, T. Yamamoto, Y. Nagata, T. Ohmura and M. Suginome, *J. Am. Chem. Soc.*, 2012, **134**, 11092–11095.
32 T. Yamamoto, Y. Akai, Y. Nagata and M. Suginome, *Angew. Chem. Int. Ed.*, 2011, **50**, 8844–8847.
33 T. Yamamoto, T. Adachi and M. Suginome, *ACS Macro Lett.*, 2013, **2**, 790–793.
34 Y. Nagata, T. Nishikawa and M. Suginome, *J. Am. Chem. Soc.*, 2015, **137**, 4070–4073.
35 Y.-Z. Ke, Y. Nagata, T. Yamada and M. Suginome, *Angew. Chem. Int. Ed.*, 2015, **54**, 9333–9337.
36 Y. Nagata, T. Nishikawa and M. Suginome, *ACS Macro Lett.*, 2016, **5**, 519–522.
37 T. Miyabe, Y. Hase, H. Iida, K. Maeda and E. Yashima, *Chirality*, 2009, **21**, 44–50.
38 T. Yamamoto, R. Murakami, S. Komatsu and M. Suginome, *J. Am. Chem. Soc.*, 2018, **140**, 3867–3870.
39 T. Ikai, M. Ando, M. Ito, R. Ishidate, N. Suzuki, K. Maeda and E. Yashima, *J. Am. Chem. Soc.*, 2021, **143**, 12725–12735.
40 S. Ikeda, R. Takeda, T. Fujie, N. Ariki, Y. Nagata and M. Suginome, *Chem. Sci.*, 2021, **12**, 8811–8816.
41 Y. Nagata, R. Takeda and M. Suginome, *ACS Cent. Sci.*, 2019, **5**, 1235–1240.
42 M. Raynal, F. Portier, P. W. van Leeuwen and L. Bouteiller, *J. Am. Chem. Soc.*, 2013, **135**, 17687–17690.
43 S. Cantekin, T. F. A. de Greef and A. R. A. Palmans, *Chem. Soc. Rev.*, 2012, **41**, 6125–6138.
44 L. Brunsveld, A. P. H. J. Schenning, M. A. C. Broeren, H. M. Janssen, J. A. J. M. Vekemans and E. W. Meijer, *Chem. Lett.*, 2000, **29**, 292–293.
45 A. J. Wilson, M. Masuda, R. P. Sijbesma and E. W. Meijer, *Angew. Chem. Int. Ed.*, 2005, **44**, 2275–2279.
46 A. J. Wilson, J. van Gestel, R. P. Sijbesma and E. W. Meijer, *Chem. Commun.*, 2006, 4404.
47 M. M. J. Smulders, A. P. H. J. Schenning and E. W. Meijer, *J. Am. Chem. Soc.*, 2008, **130**, 606–611.
48 M. M. J. Smulders, I. A. W. Filot, J. M. A. Leenders, P. van der Schoot, A. R. A. Palmans, A. P. H. J. Schenning and E. W. Meijer, *J. Am. Chem. Soc.*, 2010, **132**, 611–619.
49 Y. Dorca, J. Matern, G. Fernández and L. Sánchez, *Isr. J. Chem.*, 2019, **59**, 869–880.
50 A. Desmarchelier, X. Caumes, M. Raynal, A. Vidal-Ferran, P. W. N. M. van Leeuwen and L. Bouteiller, *J. Am. Chem. Soc.*, 2016, **138**, 4908–4916.
51 J. M. Zimbron, X. Caumes, Y. Li, C. M. Thomas, M. Raynal and L. Bouteiller, *Angew. Chem. Int. Ed.*, 2017, **56**, 14016–14019.
52 Y. Li, X. Caumes, M. Raynal and L. Bouteiller, *Chem. Commun.*, 2019, **55**, 2162–2165.
53 M. A. Martínez-Aguirre, Y. Li, N. Vanthuyne, L. Bouteiller and M. Raynal, *Angew. Chem. Int. Ed.*, 2021, **60**, 4183–4191.
54 Y. Li, A. Hammoud, L. Bouteiller and M. Raynal, *J. Am. Chem. Soc.*, 2020, **142**, 5676–5688.
55 Y. Miki, K. Hirano, T. Satoh and M. Miura, *Angew. Chem. Int. Ed.*, 2013, **52**, 10830–10834.
56 S. Zhu, N. Niljianskul and S. L. Buchwald, *J. Am. Chem. Soc.*, 2013, **135**, 15746–15749.
57 R. Y. Liu and S. L. Buchwald, *Acc. Chem. Res.*, 2020, **53**, 1229–1243.
58 S. Zhu and S. L. Buchwald, *J. Am. Chem. Soc.*, 2014, **136**, 15913–15916.
59 Y. Miki, K. Hirano, T. Satoh and M. Miura, *Org. Lett.*, 2014, **16**, 1498–1501.
60 D. Niu and S. L. Buchwald, *J. Am. Chem. Soc.*, 2015, **137**, 9716–9721.
61 J. S. Bandar, M. T. Pirnot and S. L. Buchwald, *J. Am. Chem. Soc.*, 2015, **137**, 14812–14818.
62 D. Nishikawa, K. Hirano and M. Miura, *J. Am. Chem. Soc.*, 2015, **137**, 15620–15623.
63 S.-L. Shi and S. L. Buchwald, *Nat. Chem.*, 2015, **7**, 38–44.

64 Y. Yang, S.-L. Shi, D. Niu, P. Liu and S. L. Buchwald, *Science*, 2015, **349**, 62–66.
65 Y. Xi, T. W. Butcher, J. Zhang and J. F. Hartwig, *Angew. Chem. Int. Ed.*, 2016, **55**, 776–780.
66 S. Zhu, N. Niljianskul and S. L. Buchwald, *Nat. Chem.*, 2016, **8**, 144–150.
67 S.-L. Shi, Z. L. Wong and S. L. Buchwald, *Nature*, 2016, **532**, 353–356.
68 H. Wang, J. C. Yang and S. L. Buchwald, *J. Am. Chem. Soc.*, 2017, **139**, 8428–8431.
69 S. Ichikawa, S. Zhu and S. L. Buchwald, *Angew. Chem. Int. Ed.*, 2018, **57**, 8714–8718.
70 Q.-F. Xu-Xu, Q.-Q. Liu, X. Zhang and S.-L. You, *Angew. Chem. Int. Ed.*, 2018, **57**, 15204–15208.
71 S. Guo, J. C. Yang and S. L. Buchwald, *J. Am. Chem. Soc.*, 2018, **140**, 15976–15984.
72 J. Lee, S. Radomkit, S. Torker, J. del Pozo and A. H. Hoveyda, *Nat. Chem.*, 2018, **10**, 99–108.
73 F. Xie, B. Shen and X. Li, *Org. Lett.*, 2018, **20**, 7154–7157.
74 X.-J. Dai, O. D. Engl, T. León and S. L. Buchwald, *Angew. Chem. Int. Ed.*, 2019, **58**, 3407–3411.
75 L. Yu and P. Somfai, *Angew. Chem. Int. Ed.*, 2019, **58**, 8551–8555.
76 S. Ichikawa, X.-J. Dai and S. L. Buchwald, *Org. Lett.*, 2019, **21**, 4370–4373.
77 Q.-F. Xu-Xu, X. Zhang and S.-L. You, *Org. Lett.*, 2019, **21**, 5357–5362.
78 S. Ichikawa and S. L. Buchwald, *Org. Lett.*, 2019, **21**, 8736–8739.
79 S. Feng, H. Hao, P. Liu and S. L. Buchwald, *ACS Catal.*, 2020, **10**, 282–291.
80 S. Guo, J. Zhu and S. L. Buchwald, *Angew. Chem. Int. Ed.*, 2020, **59**, 20841–20845.
81 G. Zhang, Y. Liang, T. Qin, T. Xiong, S. Liu, W. Guan and Q. Zhang, *CCS Chem.*, , DOI:10.31635/ccschem.020.202000434.
82 S. Nishino, K. Hirano and M. Miura, *Chem. – Eur. J.*, 2020, **26**, 8725–8728.
83 C. Chen, L. Wu, Y. Wang, L. Wu and Y. Zhang, *Synthesis*, 2020, **52**, 3415–3419.
84 G. Lu, R. Y. Liu, Y. Yang, C. Fang, D. S. Lambrecht, S. L. Buchwald and P. Liu, *J. Am. Chem. Soc.*, 2017, **139**, 16548–16555.
85 A. A. Thomas, K. Speck, I. Kevlishvili, Z. Lu, P. Liu and S. L. Buchwald, *J. Am. Chem. Soc.*, 2018, **140**, 13976–13984.
86 A. Desmarchelier, M. Raynal, P. Brocorens, N. Vanthuyne and L. Bouteiller, *Chem Commun*, 2015, **51**, 7397–7400.
87 A. Desmarchelier, B. G. Alvarenga, X. Caumes, L. Dubreucq, C. Troufflard, M. Tessier, N. Vanthuyne, J. Idé, T. Maistriaux, D. Beljonne, P. Brocorens, R. Lazzaroni, M. Raynal and L. Bouteiller, *Soft Matter*, 2016, **12**, 7824–7838.
88 X. Caumes, A. Baldi, G. Gontard, P. Brocorens, R. Lazzaroni, N. Vanthuyne, C. Troufflard, M. Raynal and L. Bouteiller, *Chem Commun*, 2016, **52**, 13369–13372.
89 G. Vantomme, G. M. ter Huurne, C. Kulkarni, H. M. M. ten Eikelder, A. J. Markvoort, A. R. A. Palmans and E. W. Meijer, *J. Am. Chem. Soc.*, 2019, **141**, 18278–18285.
90 E. Weyandt, M. F. J. Mabesoone, L. N. J. de Windt, E. W. Meijer, A. R. A. Palmans and G. Vantomme, *Org. Mater.*, 2020, **02**, 129–142.
91 S. Allenmark, *Chirality*, 2003, **15**, 409–422.
92 S. Tobisch, *Chem. – Eur. J.*, 2016, **22**, 8290–8300.
93 M. W. Gribble, M. T. Pirnot, J. S. Bandar, R. Y. Liu and S. L. Buchwald, *J. Am. Chem. Soc.*, 2017, **139**, 2192–2195.
94 L. Hong, W. Sun, D. Yang, G. Li and R. Wang, *Chem. Rev.*, 2016, **116**, 4006–4123.
95 M. Vaquero, L. Rovira and A. Vidal-Ferran, *Chem. Commun.*, 2016, **52**, 11038–11051.